Article:
Fernandes, J.S., Gentile, P., Martins, M. et al. (2016) Reinforcement of poly-l-lactic acid electrospun membranes with strontium borosilicate bioactive glasses for bone tissue engineering. Acta Biomaterialia, 44. pp. 168-177. ISSN: 1742-7061

https://doi.org/10.1016/j.actbio.2016.08.042

Reinforcement of Poly-L-lactic acid Electrospun Membranes with Strontium Borosilicate Bioactive Glasses for Bone Tissue Engineering

João S. Fernandes[1,2], Piergiorgio Gentile[3], Margarida Martins[1,2], Nuno M. Neves[1,2], Cheryl Miller[3], Aileen Crawford[3] Ricardo A. Pires[1,2,*], Paul Hatton[3,*], Rui L. Reis[1,2]

[1] 3B's Research Group - Biomaterials, Biodegradables and Biomimetics, University of Minho, Headquarters of the European Institute of Excellence on Tissue Engineering and Regenerative Medicine, AvePark, 4806-909 Taipas, Guimarães, Portugal

[2] ICVS/3B's - PT Government Associate Laboratory, Braga/Guimarães, Portugal

[3] Centre for Biomaterials and Tissue Engineering, School of Clinical Dentistry, University of Sheffield, Claremont Crescent, Sheffield S10 2TA, United Kingdom

* Corresponding Authors:

Ricardo A. Pires. E-mail: rpires@dep.uminho.pt

Tel: +351 253 510 907

Fax: +351 253 510 909

and

Prof Paul V. Hatton. E-mail: paul.hatton@sheffield.ac.uk

Tel: +44 (0) 114 271 7938

Fax: +44 (0) 114 226 5484

Abstract

Herein, for the first time, we combined poly-L-Lactic acid (PLLA) with a strontium borosilicate bioactive glass (BBG-Sr) using electrospinning to fabricate a composite bioactive PLLA membrane loaded with 10 % (w/w) of BBG-Sr glass particles (PLLA-BBG-Sr). The composites were characterised by scanning electron microscopy (SEM) and microcomputer tomography (μ-CT), and the results showed that we successfully fabricated smooth and uniform fibres (1 to 3 μm in width) with a homogeneous distribution of BBG-Sr microparticles (< 45μm). Degradation studies (in phosphate buffered saline) demonstrated that the incorporation of BBG-Sr glass particles into the PLLA membranes increased their degradability and water uptake with a continuous release of cations. The addition of BBG-Sr glass particles enhanced the membrane's mechanical properties (69 % higher Young modulus and 36 % higher tensile strength). Furthermore, cellular *in vitro* evaluation using bone marrow-derived mesenchymal stem cells (BM-MSCs) demonstrated that PLLA-BBG-Sr membranes promoted the osteogenic differentiation of the cells as demonstrated by increased alkaline phosphatase activity and up-regulated osteogenic gene expression (*Alpl, Sp7* and *Bglap*) in relation to PLLA alone. These results strongly suggest that the composite PLLA membranes reinforced with the BBG-Sr glass particles have potential as an effective biomaterial capable of promoting bone regeneration.

Key words: Strontium borosilicate glasses, PLLA membranes, mineralisation, osteogenic differentiation, BM-MSCs

1. Introduction

The development of biomaterials for guided bone tissue engineering (BTE) has been a hot topic of research in recent years. Biomaterials can act as a short-term template in which cells proliferate and deposit extracellular matrix (ECM), helping bone ingrowth as a part of its regeneration process. A suitable biomaterial for BTE should present appropriate mechanical properties that is able to withstand the mechanical stress occurring at the lesion site and to support cell ingrowth as part of the bone formation process. The capacity to shape the biomaterial substrate to fit exactly in the bone lesion is of particular relevance, too [1, 2].

Electrospinning is a versatile technique that applies electrostatic forces to manufacture ultrathin fibre meshes from melted polymers or polymer solutions. This methodology has been used to obtain biomaterials composed by micro- or nano-fibres with high surface areas and mechanical properties suitable for BTE by playing with its different processing parameters [2, 3]. Furthermore, electrospun membranes closely mimic the ECM promoting cell attachment and proliferation [4].

Poly-L-lactic acid (PLLA) is a biodegradable and biocompatible polymer, widely investigated for BTE, specially due to the approval of different PLLA medical devices for clinical use by the US Federal Food and Drug Administration (FDA) [5]. Furthermore, PLLA has appropriate flexibility and deformation capacity, and can be processed by different techniques (e.g. melt, dry and wet spinning, as well as electrospinning) [6-9]. However, PLLA is not commonly considered osteoinductive [4, 10]. Thus, in order to improve the biological performance of PLLA fibres, the polymeric matrix can be combined with inorganic materials, such as bioactive glasses (BG) and glass-ceramics, improving its osteoinductive potential [11, 12]. Moreover, the

PLLA degradation rate can be shaped by several different variables (e.g. chemical structure and crystallinity of the polymer, size and shape of the final material), although, the matching of the rate of degradation and the kinetics of the formation of new bone tissue is still difficult to achieve [13, 14]. The addition of an inorganic phase allows a better control of the degradation rate of the final PLLA-glass composite, which can be used to manufacture a composite with a suitable degradation rate while progressively being substituted by the new bone that is being formed [15].

Bioactive glasses (BGs) are a group of inorganic bioactive materials that are able to form a bone-like hydroxyapatite (HA) layer on their surface capable to strongly bond to hard and soft tissues [11, 16-18]. Immediately after the launch of the 45S5 Bioglass® in the market (chemical composition by mol: $0.45SiO_2 \cdot 0.06P2O5 \cdot 0.245Na_2O \cdot 0.245CaO$) it became the gold standard for bioactive glass materials [16]. Subsequently, a wide range of BGs based on the 45S5 composition have been developed and studied for BTE [19, 20]. The addition of borate glass forming units is one approach that has potential to lower melting temperatures while controlling bio-degradation and increasing conversion rates to HA [21, 22]. Borosilicate-based BGs (BBGs) have previously been studied as biomaterials and have shown relevant capacity as osteointegrative antibacterial materials to be used in BTE [23, 24]. BBGs have been also incorporated into scaffolds: Wang *et al.* [25] successfully incorporated copper doped borosilicate glasses (BBG-Cu) into a polymeric scaffold for tissue engineering purposes. They observed an improvement in the stability of the glass network and the BBG-Cu promoted the angiogenesis in rat calvarial defects.

Moreover, in our previous studies we tested a BBG glass composition (e.g. molar ratio: BBG-Sr: $0.05Na_2O \cdot 0.35SrO \cdot 0.20B_2O_3 \cdot 0.40SiO_2$) for their osteogenic capacity. We found that the presence of BBG-Sr glass particles improved the osteogenic

differentiation of bone marrow mesenchymal stem cells (BM-MSCs) and induced also the formation of mineralised tissue. We also demonstrated that demonstrated that BBG-Sr, at concentrations ≥ 18 mg/mL it was able to eradicate *Pseudomonas aeruginosa* bacterium [26]. Numerous reports have already associated Sr^{2+} with bone therapeutic potential [19]. Depending on the concentration Sr^{2+} can exerts many effects on bone metabolism at the tissue and cellular levels as well as in bone formation *in vivo* [27, 28]. For instance, Marie *et al*. [27] demonstrated strontium modulates bone cell function (e.g. cell proliferation and differentiation) *in vitro* stimulating bone formation and inhibiting bone resorption. Moreover, Hesaraki *et al*. showed that glasses doped with Strontium promoted osteoblast proliferation and ALP activity when directly in culture with cells [29]. For instance, Wu *et al*. [30] developed a strontium silicate glass which promoted a high ALP activity in BM-MSC cell culture, which was associated with the release of Sr^{2+} and silica. Also, Santocildes-Romero *et al*. [31] demonstrated that strontium-substituted bioactive glasses promoted osteogenic differentiation of BM-MSCs cultures in the presence of strontium -containing BGs. They showed an increased expression of genes such as *Alpl* and *Bglap*. Moreover, Gentleman *et al*. [32] studied the effect of the release of Si- and Sr-related chemical entities from PCL-SrBG scaffolds, and they detected that the SrBG particles stimulated osteoblast proliferation and ALP activity in relation to the SrBG-free PCL scaffold. Moreover, BM-MSCs are of special interest due to their capacity to differentiation into different lineages (including osteoblastic cells) with appropriate external stimuli and the fact that it is relatively easy to isolate [33]. For that reason, BM-MSCs have received extensive attention as promoters of tissue regeneration.

To our knowledge, the PLLA-BBG-Sr composite membranes fabricated by electrospinning has not been achieved to-date. Therefore, we aimed to evaluate the

potential of PLLA-BBG-Sr composite membranes for BTE and bone regeneration. Herein, we investigated the impact of the incorporation of BBG-Sr glass particles in PLLA fibre meshes on their tensile strength and degradation. Moreover, we evaluated the response of BM-MSCs in the presence of PLLA-BBG-Sr fibres, namely in what regards their morphology, proliferation and ability to induce its differentiation.

2. Experimental

2.1. Materials

All chemicals used for the melt-quenched synthesis were reagent grade: boron oxide (B_2O_3, Alfa Aesar, Germany), calcium carbonate ($CaCO_3$, Sigma-Aldrich, UK), sodium bicarbonate ($NaHCO_3$, Sigma-Aldrich, Australia), silica gel 60M (SiO_2, Macherey-Nagel, Germany), magnesium oxide (MgO, Sigma-Aldrich, UK) and strontium carbonate ($SrCO_3$, Sigma-Aldrich, Australia). All the chemical reagents used for electrospinning were reagent grade: PLLA with a L-lactide content of 99.6 % and an average M_w of 69,000 $g.mol^{-1}$ (Cargill Dow LLC, USA), dichloromethane (Sigma-Aldrich, UK), and the anionic surfactant docusate sodium salt (Sigma-Aldrich, UK).

The BBGs were produced as described elsewhere. Briefly, the appropriate amounts of SiO_2, B_2O_3, $NaHCO_3$, and $CaCO_3$ or MgO or $SrCO_3$, were accurately mixed with ethanol (Sigma, Portugal) in a porcelain pestle and mortar, fully dried overnight and transfer to a platinum crucible (ZGS platinum, Johnson Matthey, UK). Each batch (~ 50 g) was heated to 1450 ºC in air for 1 hour and, subsequently, the melt was quickly poured into an ice-water bath at ~ 0 ˚C to form a glass frit. Afterwards, the glasses of general formula $0.05Na_2O \cdot x MgO \cdot y CaO \cdot (0.35\text{-}x\text{-}y)SrO \cdot 0.20B_2O_3 \cdot 0.40SiO_2$ (molar ratio, where x, y = 0.35 or 0.00, and $x \neq y$) were ground into an Agate mortar (RETSCH, Germany) to obtain microparticles and sieved to a size <45 μm to be homogeneously

incorporated in the polymeric matrix during the fabrication of the fibres. The density of the BBGs was measured by a Multi pycnometer (Quantachrome Instruments, USA) under helium at 110 °C using ~ 5 g of each sample.

2.2. Glasses synthesis and membranes preparation

Electrospinning. PLLA-BBG-Sr membranes were fabricated inside a fume hood cabinet for safe solvent evaporation and in order to prevent that the turbulent air interferes in the formation of the fibres. The PLLA concentration, the ratio of PLLA/ BBG-Sr and the process parameters (e.g. applied voltage, flow rate and distance from the collector) were optimized in order to obtain uniform membrane of fibres. The final electrospun membranes were fabricated using PLLA dissolved in dichloromethane (16 % w/v) where the BBGs microparticles were suspended (10 % w/w BBGs/PLLA). Docusate sodium salt (1.2 % w/w relative to PLLA) was used to help the homogenization of the solution avoiding the formation of agglomerates. The PLLA and PLLA-BBG-Sr solutions were stirred overnight and sonicated 5 min before use to remove air bubbles. The set up was mounted using a high voltage supplier, a syringe pump (Baxter AS50) with a 20 gauge metal needle (Fisnar, New Jersey, USA) and a conductive collector. The PLLA and PLLA-BBG-Sr solutions were drawn up into a 1 ml syringe (BD Plastipak, New Jersey, USA). The solutions were electrospun using 17 kV and a flow rate of 3 mL/h at a 19 cm distance between the collector and needle. The electrospun membranes were dried in a fume hood, at room temperature, for 24 h, collected and stored in a desiccator at room temperature.

2.3. Characterisation of electro-spun membranes

2.3.1. Scanning electron microscopy (SEM)

The Scanning Electron Microscopy (Leica Cambridge S360 microscope, equipped with an energy dispersive spectrometer, UK) was used to assess the surface morphology of the fabricated PLLA and PLLA-BBG-Sr membranes. Prior to the analysis, all the scaffolds were sputter-coated with gold. The micrographs were acquired using a beam energy of 5.0kV and working distance (WD) of ~ 5.2 mm.

2.3.2. Micro-computed tomography (μCT)

Micro-computed tomography (μ-CT) was carried out on a high-resolution μ-CT scanner (SkyScan1272, Bruker, Kontich, Belgium), using a pixel size of 9.8 μm and integration time of 160 ms. The X-ray source was set at 50 kV of energy and 200 μA of current. Approximately 400 projections were acquired over a rotation range of 180° with a rotation step of 0.60°. Data sets were reconstructed using standardised cone-beam reconstruction software (NRecon v1.6.10.2, SkyScan). The output format for each sample was a series of 601 bitmap images (1224 × 1224 pixels). 3D virtual models of representative regions in the bulk of the scaffolds were created applying colour channel thresholds and visualised using an image processing software (CTvox).

2.3.3. Mechanical tests

Tensile strength and modulus of the PLLA and PLLA-BBG-Sr membranes were measured using a Uniaxial Universal Testing Machine (Instron 4505, USA) according to the standard ASTM D 638. The membranes were cut into strips of 50 mm length, 10 mm width and 0.1 mm thickness. The tests were conducted using a 1 kN load cell, with a gauge length of 20 mm and a crosshead speed of 5 $mm.min^{-1}$ until rupture. The tensile force was taken from the stress-strain curves as the maximum stress hold by the samples. Tensile modulus was estimated from the initial slope of the stress–strain curve

(between 0.5 % and 1 % strain) using the linear regression method. The average and standard deviations were determined using 5 specimens per composition.

2.3.4. Degradation assay

The electrospun membranes (n= 3 per time point) were immersed in PBS (Sigma-Aldrich, UK) at a ratio of 10:10 (membrane (mg): PBS (mL)) for 7, 14, 21, and 28 days in a water-shaking bath at 60 rpm and 37 °C. Each immersion solution was filtered and the pH measured (Crison Instruments, Spain). Inductive coupled plasma (ICP) analysis was performed to determine the concentrations of Si, B and Sr in solution. The absorption was measure at specific wavelengths (λ= 251.611 nm for Si, λ= 249.773 nm for B and λ= 407.771 nm for Sr) and the concentrations were determined using calibration curves obtained with standard solutions (Alfa Aesar) prior to the analysis of the samples.

The membranes were removed from PBS, the excess surface water was removed and the samples were immediately weighed. Afterwards, the samples were dried in the oven at 37 °C, to constant weight, recording the final mass of the membranes. The water uptake (WU) was calculated according to Eq. (1):

$$WU(\%) = (m_{tp} - m_f)/m_f \times 100 \quad \text{Eq. (1)}$$

Where m_{tp} is the wet mass of the specimen at the specific time (days), and m_f is the final mass after immersion and drying. The weight loss (WL) was calculated according to Eq. (2):

$$WL(\%) = (m_f - m_i)/m_i \times 100 \quad \text{Eq. (2)}$$

Where m_f is the mass of the dried membranes after its immersion in water, and m_i is the mass of the dried membranes before immersion in PBS.

Thermogravimetric analysis (TGA; Q500, TA Instruments, USA) was also used to quantify the changes in the weight (mass) of the membranes during the degradation process. In addition, thermal analysis was performed to determine the amount of BBG-Sr (non-combustible) glass particles that was compounded with PLLA to produce the composite membranes. Experiments were performed in platinum pans, at a heating rate of 40 k·min^{-1} from 50 to 700 °C in an oxygen atmosphere.

2.4. *In vitro* culture of BM-MSCs on electrospun membranes

2.4.1. Isolation and expansion of BM-MSCs

Bone marrow mesenchymal stem cells (BM-MSCs) were isolated from bone marrow of 4-5 week-old male Wistar rats according to the method established by Maniatopoulos *et al.* [34] and recently used by by Santocildes-Romero [31]. BM-MSCs were expanded in basal medium consisting of Dulbecco's modified Eagle's medium (DMEM; Sigma-Aldrich, UK), supplemented with 100 U/mL penicillin (Sigma-Aldrich, UK) and 100 µg/mL streptomycin (Sigma-Aldrich, UK). Cells were cultured at 37 ºC in an atmosphere of 5 % CO_2.

2.4.2. Culture of BM-MSCs

Prior to the *in vitro* studies, BM-MSCs, at passage 2, were harvested and seeded at a density of 3×10^4 cells per membrane of Ø = 6.5 mm held in plastic inserts (CellCrown™ 24, Scaffdex, UK). Cells were cultured for 7, 14 and 21 days under static conditions. All scaffold conditions were cultured in basal and osteogenic differentiation media (basal medium supplemented with 50 µg/mL L-ascorbic acid, 10 mM β-glycerophosphate and 10^{-8} M dexamethasone).

2.4.3. BM-MSCs proliferation, viability and morphology

Morphological evaluation of cultured cells: After each time-point the cells cultured on the membranes were washed with PBS and fixed with 4% formalin solution (0.5 mL) for 15 min at room temperature (RT). The cells were then washed with PBS, containing 0.2 % Triton X, for 2 min. After the fixation and permeation steps, the cells were washed again with PBS and stained with 4,6-diamidino-2-phenyindole dilactate (1:1000 DAPI, Sigma-Aldrich, UK) for 2 min at RT, and phalloidin-tetramethylrhodamine B isothiocyanate (Sigma-Aldrich, UK) for 1 h at RT. Finally, the cells were washed and observed using an Axioplan 2 imaging fluorescent microscope with a digital camera QIC AM 12-bit (Zeiss, UK).

Cell viability and proliferation (PrestoBlue® and PicoGreen® assays). The PrestoBlue® reagent (Fisher Scientific, UK) is a resazurin-based solution that is reduced to resorufin by viable cells which can be detected flurometrically. The cell viability assay was executed according to the manufacturer's instructions. In brief, the PrestoBlue® reagent was added to a final concentration of 10 % to the cell culture medium and the cultures incubated for 1 h at 37 ^{o}C. 200 µL samples of the culture medium were removed and placed in 96-well plates and the resorufin fluorescence quantified spectrophotometrically using a plate reader (Tecan Infinite M200). The fluorescence was determined at an excitation wavelength of 560 nm and emission wavelength of 590 nm. The metabolic activity was presented in fluorescence values and compared with the control (cell cultured onto PLLA membranes under basal medium conditions).

The PicoGreen® dsDNA reagent (Invitrogen, USA) is an ultrasensitive fluorescent nucleic acid dye for quantification of double-stranded DNA (dsDNA) in solution. This assay enables measurement of cell proliferation. After each culturing period, the cells were washed with PBS and incubated at 37 ºC for 3 h followed by a freezing step at -80

259 ºC for overnight in ultra-pure water (1 mL) to ensure the cell lysis. Finally, the
260 fluorescence was determined at an excitation wavelength of 485 nm and emission
261 wavelength of 528 nm. The DNA concentration was presented in µg/mL and compared
262 with the control (cell cultured onto PLLA membranes under basal medium conditions).

263 **2.4.3. Alkaline phosphatase quantification**

264 The concentration of alkaline phosphatase (ALP) was determined for all the cell culture
265 time points, using the lysates used for the DNA quantification and the Alkaline
266 Phosphatase, Diethanolamine Detection kit (Sigma-Aldrich, UK), which is based on the
267 conversion of p-nitrophenyl phosphate (pNPP) to free p-nitrophenol by ALP. In brief, a
268 buffered pNPP solution was prepared and equilibrated at 37 ºC. Afterwards, 2 % (v/v)
269 of sample or control lysate was added. Immediately after mixing the absorbance was
270 read at 405 nm in a plate reader (Tecan Infinite M200) for ≈ 5 min. An ALP standard
271 solution was used as control and buffer as blank. The units were calculated according to
272 the following Eq. (3):

273 $$\frac{(\Delta A_{405nm}/\min\ Test - \Delta A_{405nm}/\min\ Blank)\times df \times V_F}{18.5\times V_E} \quad \text{Eq. (3)}$$

274 Where df = dilution factor; V_F = Volume of final solution; 18.5 = millimolar extinction
275 coefficient of pNPP at 405 nm and V_E = Volume of samples/ALP standard solution.

276 **2.4.4. RNA isolation and real-time quantitative polymerase chain reaction (rtPCR)**

277 RNA was extracted with Tri-reagent (Sigma-Aldrich, UK) according to the
278 manufacturer's instructions. The RNA concentration was determined by
279 microspectrophotometry (NanoDrop 1000). The cDNA synthesis was performed using
280 the qScript cDNA synthesis kit (Quanta BioSciences, VWR) with 100 ng of RNA
281 template in a final volume of 20 µL. Cycling was as follows: 1 cycle at 22 °C, 5 min; 1

cycle at 42 °C, 30 min; 1 cycle at 85 °C, 5 min. The amplification of the target cDNA was performed using the PerfeCTa SYBR Green FastMix (Quanta BioSciences) with 1 µL of cDNA, 200 nM of each primer (**Table 1**) in a final volume of 20 µL. Real time-PCR cycling was as follows: 1 cycle at 95 °C, 2 min; 44 cycles at 95 °C; 10 s at gene annealing temperature (**Table 1**); 30 s at 72 °C; followed by dissociation curve analysis. All the reactions were carried out on a PCR cycler Mastercycler Realplex (Hamburg, Germany). The transcripts expression data were normalized to the housekeeping gene glyceraldehyde-3-phosphate dehydrogenase (*Gapdh*) in each sample. The quantification was performed according to the Livak method ($2^{-\Delta\Delta Ct}$ method [35]), considering as calibrator at each time point the PLLA - basal medium for PLLA- osteogenic medium and PLLA-BBG-Sr basal medium for PLLA-BBG-Sr osteogenic medium (threshold = 1).

Table 1. Primers used for qPCR

Gene	Primer sequence 5'-3' Forward/ reverse	Tm (ºC)
Osteocalcin (*Bglap*)	CATCTATGGCACCACCGTTT AGAGAGAGGGAACAGGGAGG	60.0
Osteopontin (*Spp1*)	ATCTCACCATTCCGATGAATCT CAGTCCATAAGCCAAGCTATCA	60.0
Osterix (*Sp7*)	CACTGGCTCCTGGTTCTCTC CCACTCCTCCTCTTCGTGAG	60.0
Alkaline phosphatase (*Alpl*)	TGCCTTACCAACTCATTTGTG ACGCGATGCAACACCACTC	57.4

3. Results and discussion

3.1. Characterisation of electrospun membranes

The PLLA and PLLA-BBG-Sr (10 % w/w BBG-Sr/PLLA) composite membranes were successfully obtained by electrospinning. TGA analysis confirmed that we successfully incorporated 10 % (w/w) of BBG-Sr microparticles in the PLLA fibres. The morphology, microstructure and fibre integrity of the electrospun PLLA and PLLA-BBG-Sr membranes was characterised by scanning electron microscopy (SEM) and μCT. Electrospun PLLA and PLLA-BBG-Sr membranes are composed of smooth and uniform fibres. No large particles were detected (**Figure 1**a and 1c), however, the formation of small agglomerates in the membranes containing the BBG-Sr microparticles was observed [36]. **Figure 1**c highlights in red circles the BBG-Sr microparticles incorporated into the fibres. The homogeneous distribution of the BBG-Sr microparticles in the PLLA-BBG-Sr membrane could be observed in the 2D virtual model representatively obtained using an image processing software CTvox of μCT images (**Figure 1**d), in which the red colour represents the BBG-Sr microparticles distributed into the composite membranes in green. As expected, the PLLA membranes do not present any particles in their structure (**Figure 1**b).

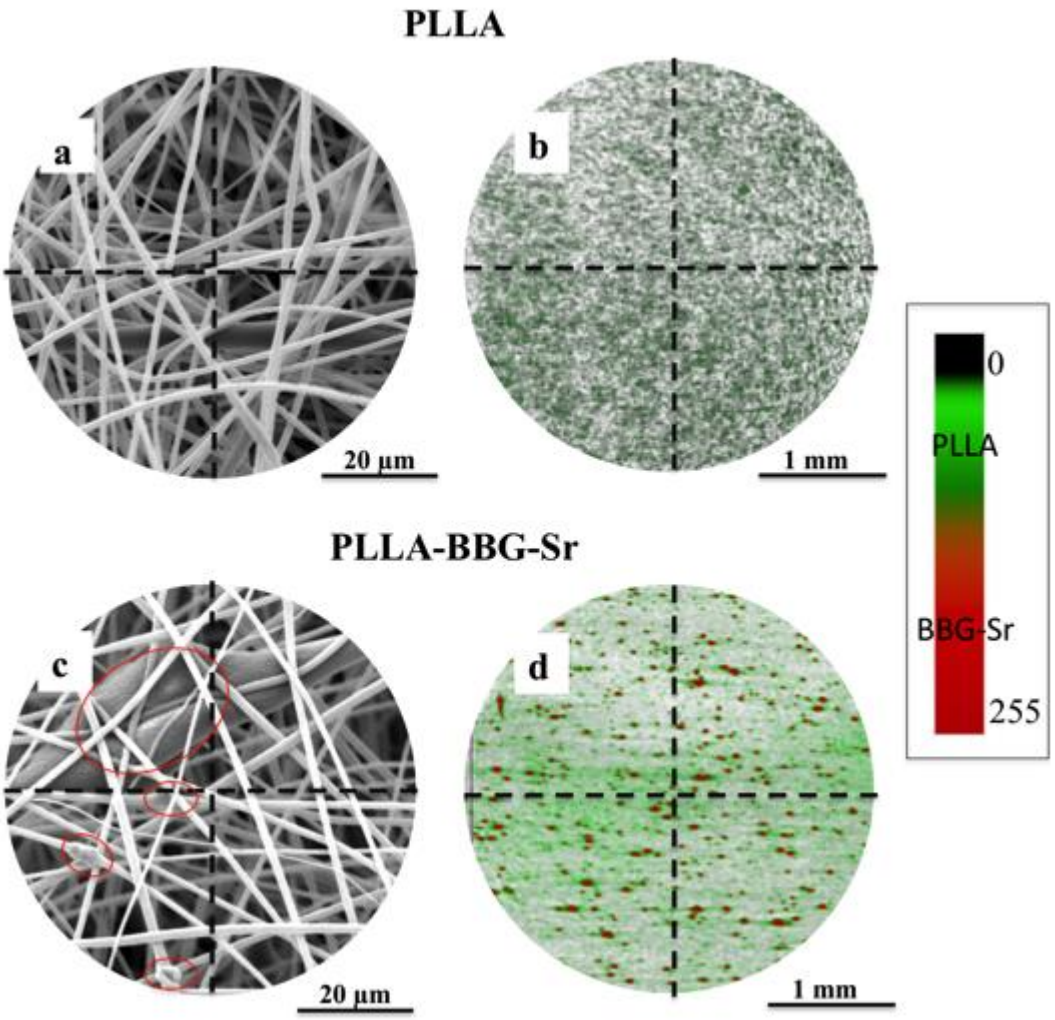

313

314 **Figure 1.** SEM micrographs (a and c) and representative µCT 2D images (b and d) of
315 PLLA and PLLA-BBG-Sr membranes. The areas encompassed by red lines in (c) show
316 particles incorporated into the fibres. In (b and d) PLLA fibres are represented in green
317 and the BBG-Sr microparticles are represented in red.

318 The mechanical properties of the biomaterials are important in providing physical
319 support for cell growth and migration matching those of the tissue at the site of
320 implantation [37]. **Figure 2**a presents the stress–strain curves obtained for the PLLA
321 and PLLA-BBG-Sr membranes under tensile load up to a strain of 50 %. The PLLA-
322 BBG-Sr membranes showed the highest tensile strength (0.75 ± 0.7 MPa), when
323 compared to the PLLA membranes (0.55 ± 0.6MPa), indicating that the incorporation

of BBG-Sr reinforced the membranes. The same trend was observed for the Young's modulus (**Figure 2**b), calculated from the initial linear slope of the stress-strain curves, where the loading of BBG-Sr microparticles improved the modulus from 14.6 ± 3.8 MPa (PLLA) to 24.7 ± 5.3 MPa (PLLA-BBG-Sr). This might be due to an increase in rigidity through the filler effect, in which the microparticles encumber the movement of the polymer chains and the amount of extendable material in the membrane. On the other hand, while the incorporation of the microparticles in PLLA-BBG-Sr membranes can affect the tensile strength, where there is no interaction between fibres and particles. The availability of cations derived from the incorporated microparticles may contribute to the crosslinking of the carboxylic acid groups (that are present in the chain ends of the PLLA) through the formation of carboxylates with the cations released from the microparticles. These carboxylate cross-links induce the interlocking of the membranes, resulting in an improvement of the Young modulus [38] As demonstrated by Thomas *et al*. [39], small concentrations of nano hydroxyapatite (HA) resulted in a reinforcement of PCL. It was observed by Jeong *et al*. [40] in an analogous way that the addition of increasing concentrations of HA increasingly enhanced the mechanical properties of the composite, namely their tensile strength and Young's modulus. Therefore, our results support that, with the inclusion of BBG-Sr microparticles into the PLLA matrix, it is possible to tune their mechanical properties, contribution to be a closer match of those from the living tissue at the site of implantation.

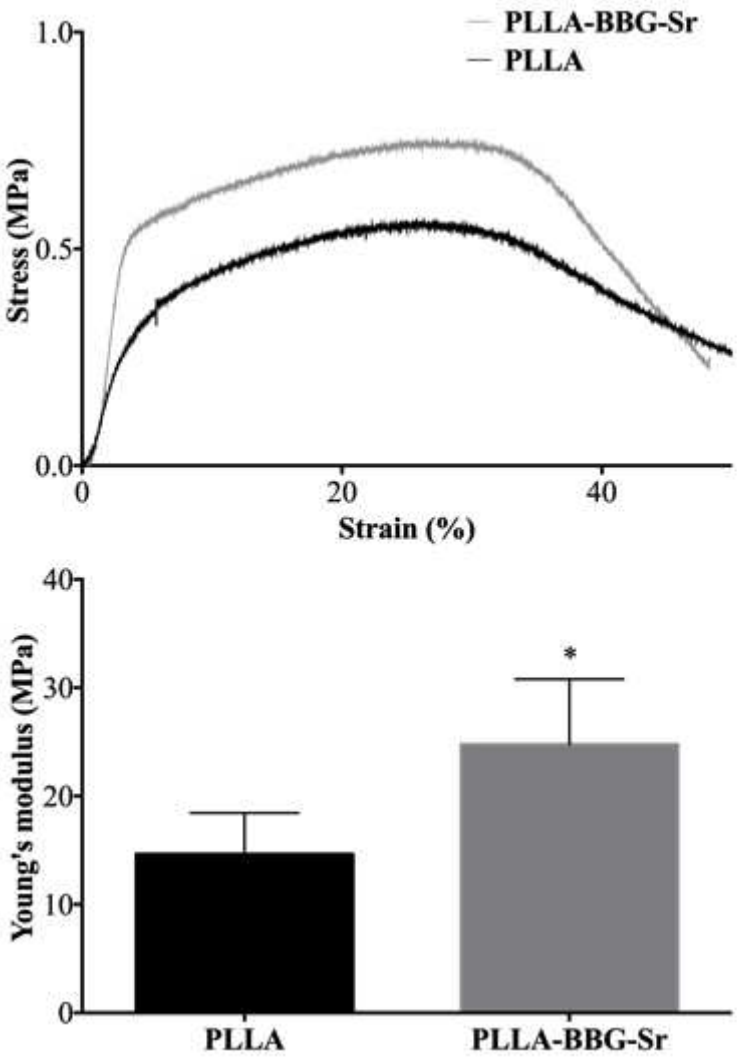

Figure 2. (a) Stress–strain curves of PLLA and PLLA-BBG-Sr membranes and their respective (b) Young's modulus determined from the initial slope of the curves. The data was analysed by non-parametric statistics: Mann-Whitney test revealed a significance of $p<0.05$ (*).

3.2. Degradation of the electrospun membranes

A biomaterial suitable for promoting bone regeneration in a tissue engineering perspective should present an appropriate biodegradability. The BTE concept is based on the substitution of the biomaterial by new bone. This requires that the degradation

rate of the biomaterial matches that of new bone formation, in order to occur a progressive substitution of the biomaterial by the new bone tissue [15, 41]. The degradation profiles of PLLA and PLLA-BBG-Sr membranes (**Figure 3**) were evaluated from the weight loss and water uptake, as well as the release of chemical species from the membranes and pH of the immersion solutions. The water uptake and weight loss data showed differences between the PLLA and the PLLA-BBG-Sr membranes (**Figure 3**a and b). Both membranes presented steady and continuous water uptake and weight loss from week 2 to week 3. However, the PLLA-BBG-Sr membranes presented a more pronounced 'burst' of weight loss during the first week. The differences between the two membranes during this initial stage of degradation might be attributed to the penetration of the PBS solution through the polymer/glass interface and/or surface cracks that facilitated the degradation of the material and enhanced the water uptake. Another possibility is related with a superficial hydrolytic degradation generated by the leaching of chemical species from the glass particles [42, 43]. The pH measurements presented no significant variation of pH for both PLLA and PLLA-BBG-Sr membranes over time. It was observed an increasing release of B, Si and Sr from the PLLA-BBG-Sr membranes over time of immersion (**Figure 3**c). The release of such chemical species can only be originated from the BBG-Sr microparticles, confirming that the weight loss is mainly caused by the hydrolytic degradation of the glass particles. During the last week of degradation (21 to 28 days) it was also noticed an increase in the PLLA-BBG-Sr weight loss that is in line with the reduction of glass content as determined by TGA tests (**Figure 3**d) and the increased concentration of mainly B and Sr-containing chemical species, that were leached from the glass particles to the immersion medium (detected by ICP). The increase on the degradation is clear during the last week; however, the leaching observed by ICP during

379 the first 3 weeks is not corroborated by the TGA analysis. In this case, the presence of
380 phosphates from the solution buffer might generate a surface layer of strontium
381 phosphate that limits the mass exchange from the glass particles to the immersion
382 solution. In this case, the weight loss derived from the leaching of B, Si and Sr from the
383 glass particles is partially compensated by the deposition of phosphates. The fact that
384 the PLLA-BBG-Sr composite membranes lost twice the mass during the degradation
385 process suggests that the incorporation of BBG-Sr into PLLA fibres increased the
386 degradability and the degradation rate of the membranes, as well as the release of active
387 chemical species to the surrounding medium [15].

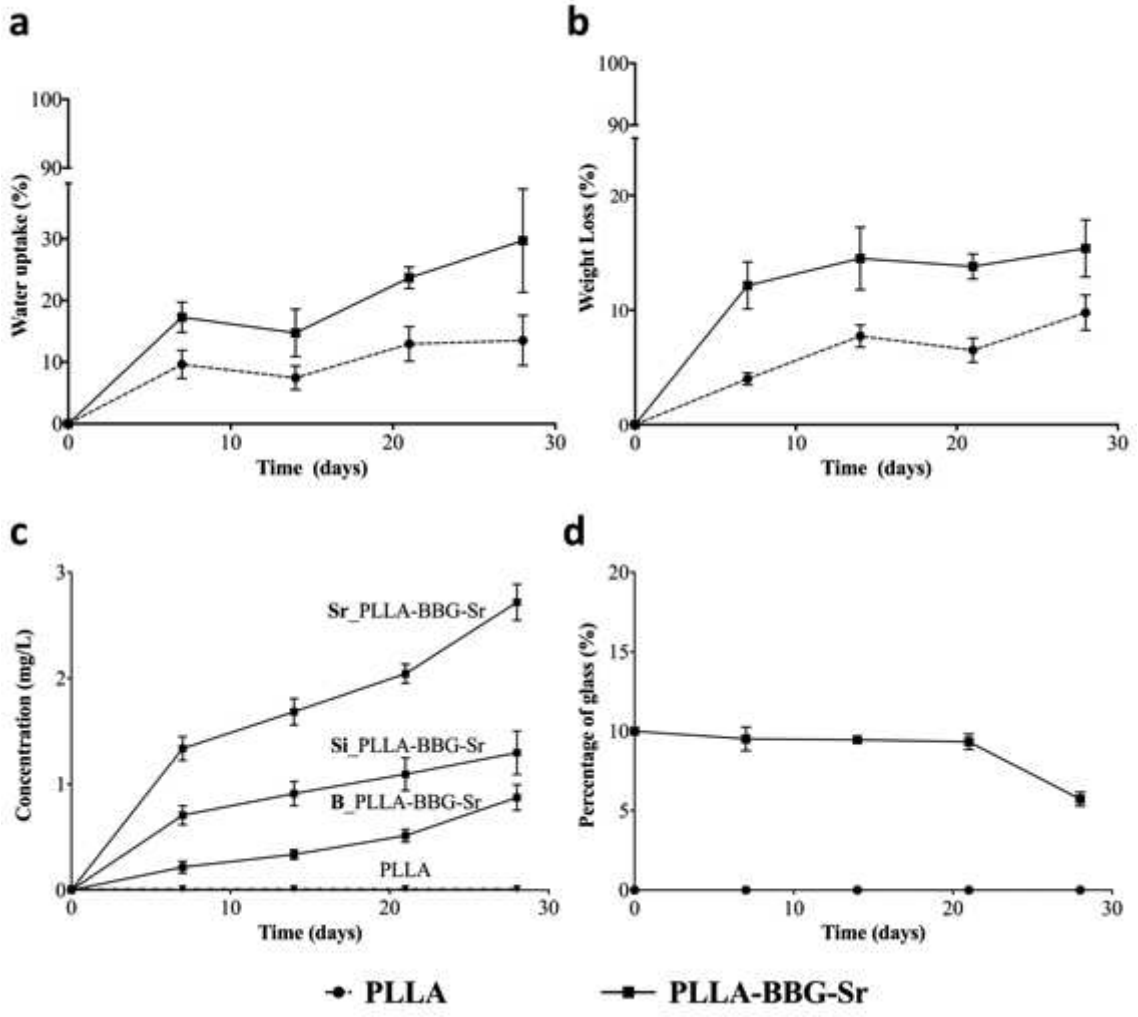

388

389 **Figure 3.** Degradation profile of the PLLA and PLLA-BBG-Sr membranes during 30
390 day of degradation in PBS at 37 ºC. (a and d) WU and WL of the PLLA and PLLA-
391 BBG-Sr membranes; (c) release profiles of chemical species from the PLLA-BBG-Sr
392 membranes; and (d) percentage of glass (w/w) in the studied membranes.

393

394 **3.3. *In vitro* biological evaluation**

395 **Morphology, viability and proliferation of the BM-MSCs**

396 Apart from the suitable chemical and physical properties of the biomaterial, it is also
397 crucial to evaluate if theyare cytotoxic.. To this purpose, direct contact assays are

398 widely used as a preliminary screening for biomaterials [44]. Fluorescence microscopy
399 images (**Figure 4**a) show the morphology of BM-MSCs cultured in the presence of
400 PLLA and PLLA-BBG-Sr membranes in basal or osteogenic medium (**Figure 4**a, Basal
401 and Osteo, respectively). The attached BM-MSCs displayed a well-spread morphology
402 and several cell-to-cell contacts. As expected, the PrestoBlue® and PicoGreen® data
403 (**Figure 4**b and 4c) demonstrated that the cells proliferated over the time course under
404 basal conditions, which is consistent with the morphology images (**Figure 4**a). There is
405 also and increase on their metabolic activity (day 7 versus day 21). However, under
406 osteogenic conditions BM-MSCs did not proliferate and exhibited an increase
407 inmetabolic activity (day 7 versus day 21), which suggested the occurrence of
408 differentiation [8, 45]. PLLA and PLLA-BBG-Sr electrospun membranes were found to
409 be a non-cytotoxic support for BM-MSCs attachment and proliferation (**Figure 4**)
410 without any adverse effect caused by the addition of BBG-Sr particles. Inaddition, the
411 randomly distributed fibres and porous structure of electrospun membranes should
412 enable an efficient transfer of nutrients, as well as support suitable cell penetration into
413 the bulk of the membranes.

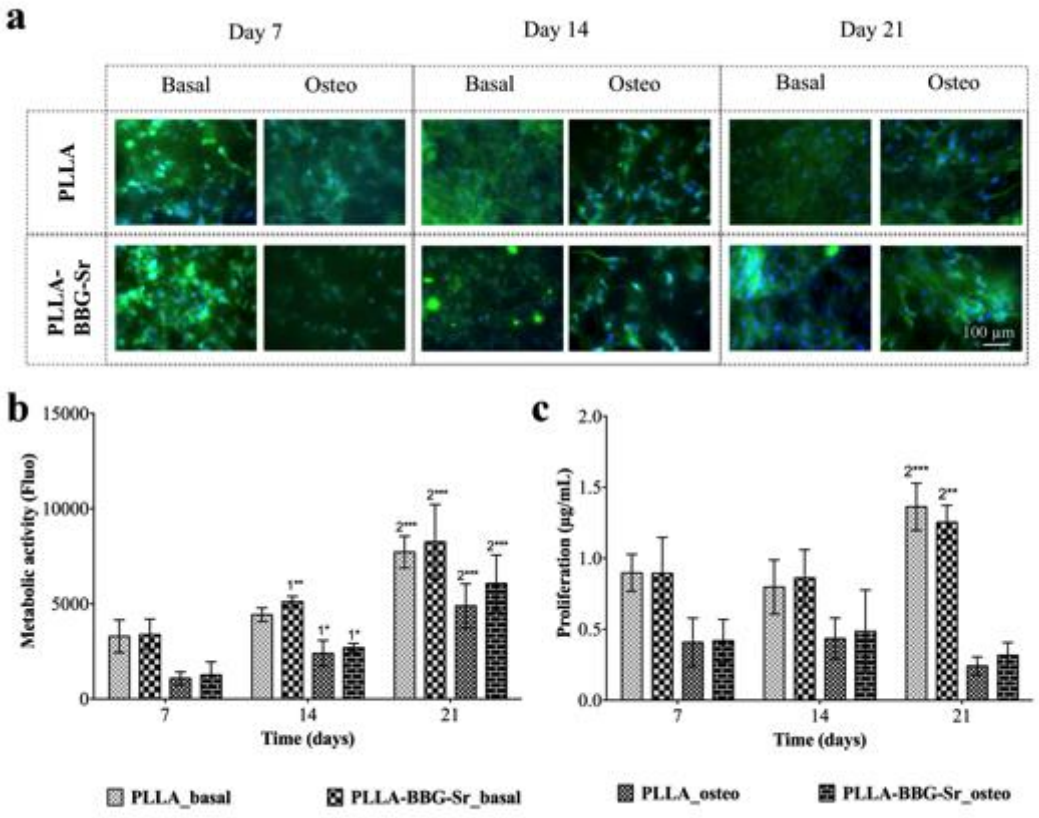

414

415 **Figure 4.** (a) Morphology, (b) metabolic activity and (c) proliferation of BM-MSCs
416 cultured for 7, 14 and 21 days in basal (basal) or osteogenic medium (osteo), and in the
417 presence of PLLA or PLLA-BBG-Sr. In the representative microscopy images (a) the
418 nuclei of cells are stained in blue (DAPI) and the actin filaments are stained in green
419 (Phalloidin). In Figure 4b and 4c, the results are expressed as means ± standard
420 deviation with n = 3 for each experimental data point. The data were analysed by non-
421 parametric statistics: Kruskal-Wallis test, followed by a Dunn's Multiple Comparison
422 test and were marked as: *** p<0.001; **p<0.01; * p<0.05. On the graphs the figure '1'
423 represents the comparison with day 7 and the figure '2' represents the comparison with
424 day 14.

425 **3.3. Osteogenic differentiation markers**

426 It has been demonstrated that the release of chemical species containing Si, B or Sr from
427 BBG-Sr glass particles could stimulate the osteoblast proliferation and differentiation.
428 The ALP activity is commonly related with functional activity of the bone-derived cells,
429 such as their osteogenic differentiation and the onset of mineralisation [36, 46]. In order
430 to execute a preliminary evaluation on the capacity of the PLLA-BBG-Sr membranes to
431 induce osteogenic differentiation, we cultured BM-MSCs onto them and quantified the
432 ALP activity after 7, 14 and 21 days (Figure 5b). SEM was also used to check for
433 mineral deposits and the mineralisation stage of the BM-MSCs (Figure 5a). In the SEM
434 micrographs it is possible to confirm that the BM-MSCs create a cell layer attached to
435 the PLLA and PLLA-BBG-Sr membranes. However, in the case of BM-MSCs cultured
436 under osteogenic conditions, formation of phosphate deposits at the later time points
437 (**Figure 5**a, day 21) were observed. In contrast, ALP activity (**Figure 5**b) increased
438 during the time of culture under osteogenic conditions, suggesting that the addition of
439 BBG-Sr microparticles increased the ALP expression levels. Therefore, the PLLA-
440 BBG-Sr membranes stimulated the BM-MSCs to initiate their osteogenic
441 differentiation. This stimulus is very likely to be related with the presence of the B, Si
442 and Sr chemical species leaching from the BBG-Sr glass particles to the surrounding
443 medium [47, 48], as also shown in the ICP data (**Figure 3**a). Comparatively, some
444 authors [31, 32] studied the effect of the release of Si and Sr chemical species from BG,
445 and found that they stimulate cell differentiation. Other authors have also demonstrated
446 improvements in cell differentiation and bone mineralisation by the addition of glass
447 particles into polymeric matrices [6, 36, 49]. As an example, Santocildes-Romero [9],
448 fabricated electrospun membranes incorporating 10% BGSr glass particles with
449 increasing Sr composition with no cytotoxic effects on at osteosarcoma cells; Rajzer
450 and co-workers [36] verified that the addition of 20% hydroxyapatite ceramic particles

into PLDL electrospun composites could direct HAp mineralisation in cell culture; Ren *et al*. [6] also showed that PCL-SrBG electrospun scaffolds enhanced the ALP activity of MC3T3-E1 cells in the presence of osteogenic media in comparison with the glass-free PCL scaffolds after 21 days of culture. Hence, the addition of BBG-Sr glass particles to PLLA fibres accelerates the BM-MSCs osteogenic differentiation (ALP activity, **Figure 5a**), in the presence of osteogenic media after 14 days of cell culture, showing an higher increase after 21 days of cell culture.

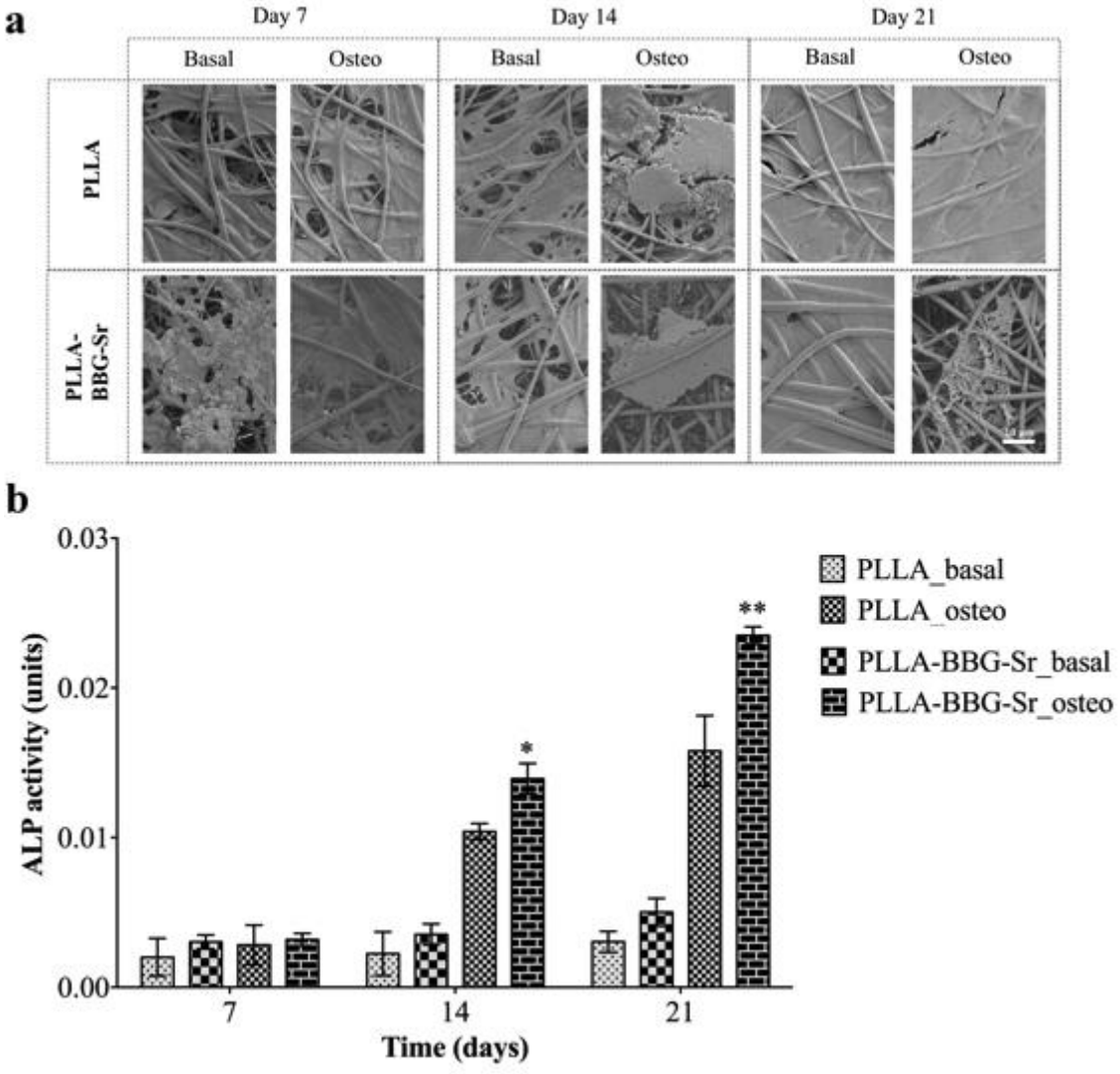

Figure 5. (a) Morphology/mineralisation (SEM micrographs) of BM-MSCs and their (b) ALP activity after 7, 14 and 21 days of culture in the presence of PLLA and PLLA-

461 BBG-Sr, in basal (basal) or osteogenic medium (osteo). ALP results are expressed as
462 mean ± standard deviation with n = 3 for each datapoint. The data was analysed by non-
463 parametric statistics: Kruskal-Wallis test, followed by a Dunn's Multiple Comparison
464 test. ** (p<0.01); * (p<0.05). The significance is in relation to cells cultured on PLLA (in
465 the absence of BBG-Sr glass particles) under the same culture conditions.

466

467 Complementary to the reported viability, proliferation and ALP activity data, the
468 differentiation level of BM-MSCs cultured onto PLLA and PLLA-BBG-Sr membranes
469 was assessed by quantitative PCR of selected bone-specific gene transcripts. In the
470 literature it is well described that osteogenic differentiation of BM-MSCs has three
471 phases: the proliferative phase, which is followed by the ECM synthesis and maturation,
472 and lastly the mineralisation phase [50, 51]. Therefore, in this study the osteogenic
473 potential of the cells was evaluated at day 14 and 21 using the expression pattern of the
474 representative osteogenic markers: *Alpl*, *Spp1*, *Bglap* and *Sp7* [8, 52]. The transcripts
475 expression data were normalized against the housekeeping gene *Gapdh* and the
476 quantification performed according to the Livak method ($2^{-\Delta\Delta Ct}$ method), considering
477 the PLLA (basal medium) as calibrator for PLLA (osteogenic medium) and PLLA-
478 BBG-Sr (basal medium) as calibrator for PLLA-BBG-Sr (osteogenic medium).
479 Commonly, *Alpl* acts as early marker of the osteoblastic phenotype. This gene
480 expression level is known to increase with the progression of osteoblastic differentiation
481 [53]. According to the gene expression data (**Figure 6**a) there is a significant up-
482 regulation of *Alpl* in the BM-MSCs cultured onto PLLA-BBG-Sr membranes at 14 and
483 21 days of culture in relation to BM-MSCs cultured onto PLLA membranes (all under
484 osteogenic medium). Again, the Ren et al. found the same *Alpl* gene up regulated in
485 MC3T3 cells cultured in PCL-SrBG membranes, but only after 21 days of culture.

These observations are consistent with the quantification of the ALP activity (**Figure 5**b), in which there was a significantly higher activity for the BM-MSCs cultured onto PLLA-BBG-Sr (under osteogenic medium) after 14 days of culture, when compared with the cells cultured onto PLLA [47, 48]. Regarding the maturation and mineralization phase, we investigated the expression of the genes that encode two non-collagenous proteins present with the ECM of bone, e.g. *Spp1* and *Bglap*. *Spp1* is a protein found in bone, teeth, kidneys and epithelial lining tissue; consequently, *Spp1* cannot be considered bone-specific, although it is associated to bone related functions [8, 45]. The *Spp1* gene expression results (**Figure 6**b) showed that at 14 days of culture, BM-MSCs cultured on PLLA presents a high *Spp1* expression, which might be related with their important functions in cell adhesion, migration and survival [53]. The fact that *Spp1* expression is significantly higher when cultured on PLLA membranes might be a result of proliferation and cell spreading processes. On the other hand, *Bglap*, which is the second most abundant protein present in bone, is exclusively secreted by osteoblastic cells at the last stage of maturation [45, 53]. When cultured on PLLA-BBG-Sr membranes, *Bglap* expression (**Figure 6**c) is significantly higher in relation to the basal medium for 14 and 21 days of culture. This suggests that the combined effect of the osteogenic factors and the dissolution products might be enhancing *Bglap* gene expression, which may be an indicator of osteoblastic differentiation. This data is in accordance with the report of Strobel *et al*. [54] showing that BM-MSCs, after 14 days of exposure to cell culture medium containing nanoparticles of Sr-substituted Bioglass, increased their *Bglap* expression. Finally, *Sp7* is a well-characterised osteoblast specific gene and it is associated with the regulation of numerous other genes (e.g. osteocalcin, osteopontin, bone sialoprotein), and is acknowledged as a late bone marker that plays a key role in the differentiation of preosteoblasts into fully functioning osteoblasts [8, 53].

Our data at day 21 registered an increase of *Sp7* gene expression in the BM-MSCs cultured on PLLA-BBG-Sr membranes (under osteogenic medium) in relation to the same cells cultured on the same membranes but under basal medium, as well as the cells cultured onto PLLA (under osteogenic and basal medium). These observations are consistent with the overexpression of the other monitored gene *Alpl* and their protein expression (ALP) for PLLA-BBG-Sr membrane [55]. In fact, Isaac *et al*. [56] demonstrated that the addition of strontium to bioactive glass particles resulted in a significant up-regulation of Runx2 and Osterix of osteoblastic cells. In summary, the detected overexpression of *Alpl, Bglap* and *Sp7* genes in cells cultured onto PLLA-BBG-Sr membranes show that the incorporation of BBG-Sr glass particles into the PLLA membranes promotes the osteogenic differentiation of BM-MSCs [47].

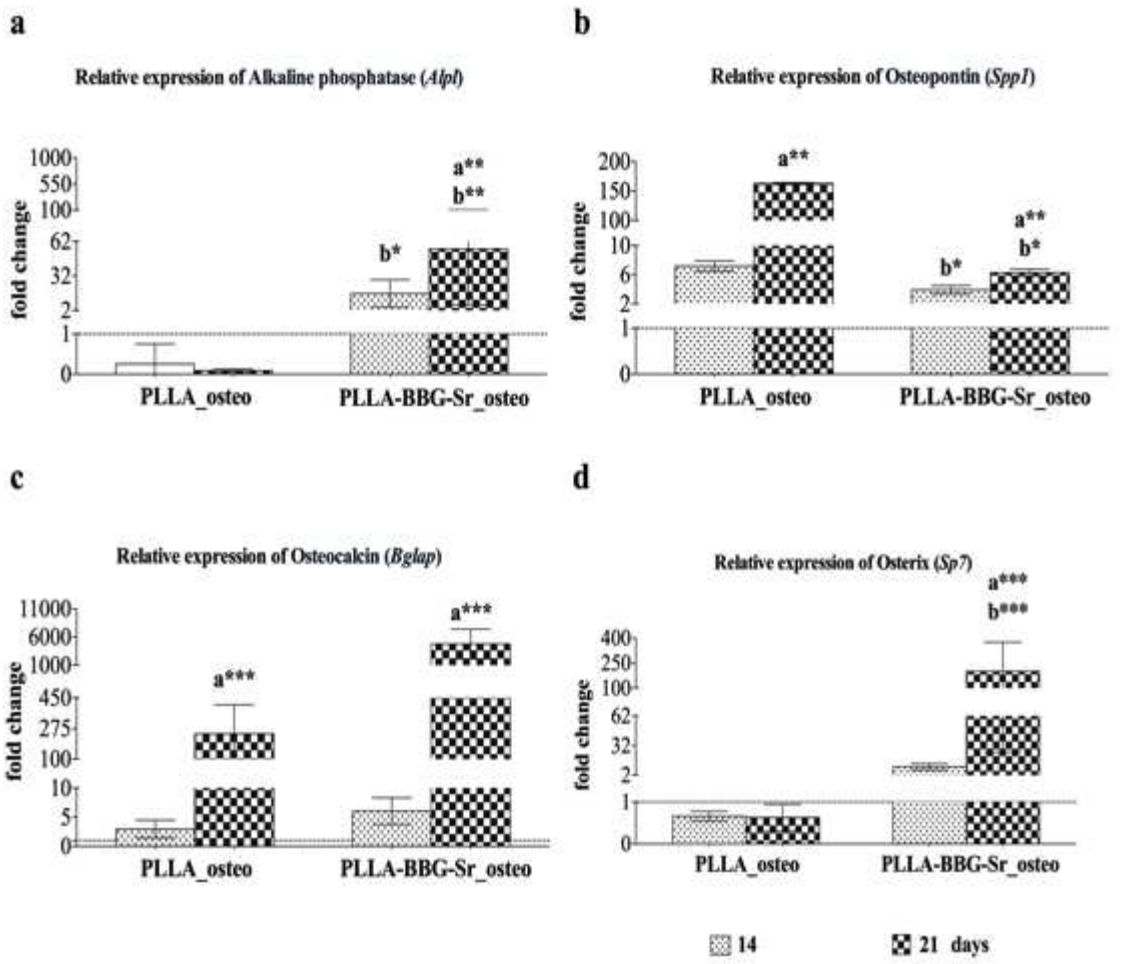

522

523 **Figure 6.** Relative gene expression profile of BM-MSCs cultured onto PLLA and
524 PLLA-BBG-Sr membranes during 14 and 21 days. Selected genes: *Alpl,* osteogenic
525 mineralisation initiators (a); *Spp1 (b)* and *Bglap (c)*, extracellular matrix; *Sp7*,
526 transcription factors. The transcripts' expression data were normalized against the
527 housekeeping gene *Gapdh* and the quantification performed according to the Livak
528 method ($2^{-\Delta\Delta Ct}$ method). For each timepoint it was used: the calibrator PLLA (in basal
529 medium) for the experiments with PLLA (in osteogenic medium); and the calibrator
530 PLLA-BBG-Sr (in basal medium) for the experiments with PLLA-BBG-Sr (in
531 osteogenic medium). In all the cases the calibrator is represented as a dashed line
532 (threshold = 1). The results are expressed as mean ± standard deviation with n = 3 for
533 each bar. The data was analysed by non-parametric statistics: Kruskal-Wallis test,

followed by a Dunn's Multiple Comparison test and differences were considered: *** $p<0.001$; ** $p<0.01$; and * $p<0.05$. *a* denotes significant differences in relation to cells cultured in basal medium (PLLA or PLLA-BBG-Sr); *b* denotes significant differences in relation to cell cultured onto PLLA in osteogenic medium.

4. Conclusion

Bioactive membranes of PLLA-BBG-Sr composites were successfully prepared using electrospinning. The μCT data evidenced that BBG-Sr microparticles were homogeneously incorporated into the fibres and the membrane structure. Our data indicated that, the addition of BBG-Sr into the PLLA matrix improved the *in vitro* water uptake and degradability of the membranes. Moreover, the incorporation of the BBG-Sr microparticles improved the mechanical properties of the membranes, namely in their Young modulus and tensile strength. The *in vitro* biological evaluation confirmed that both PLLA and PLLA-BBG-Sr membranes are able to promote the attachment of BM-MSCs, without any cytotoxic effects. Furthermore, the addition of BBG-Sr microparticles to the PLLA membranes increased the ALP activity (under osteogenic conditions), as well as the BM-MSCs osteogenic differentiation as shown by up-regulation of *Alpl*, *Sp7* and *Bglap* gene expression *in vitro*. The present work suggests that the composite of PLLA membranes and BBG-Sr microparticles can be used as a strategy to prepare bioactive composite membranes for bone regeneration.

Acknowledgements

The authors gratefully acknowledge financial support from Portuguese Foundation for Science and Technology (Ph.D. grant BD/73162/2010), the European Union's Seventh Framework Programme (FP7/2007–2013) under Grant No. REGPOT-CT2012-31633-POLARIS. This work was also supported by the European Research Council grant

558 agreement ERC-2012-ADG-20120216-321266 for the project ComplexiTE and UK
559 EPSRC Centre for Innovative Manufacturing of Medical Devices-MeDe Innovation
560 (EPSRC grant EP/K029592/1).

561

562

5. References

[1] Zhao S, Zhu M, Zhang J, Zhang Y, Liu Z, Zhu Y, Zhang, Changqing. Three dimensionally printed mesoporous bioactive glass and poly(3-hydroxybutyrate-co-3-hydroxyhexanoate) composite scaffolds for bone regeneration. Journal of Materials Chemistry B 2014;2:6106-18.

[2] Jiang T, Carbone EJ, Lo KWH, Laurencin CT. Electrospinning of polymer nanofibers for tissue regeneration. Progress in Polymer Science 2015;46:1-24.

[3] Gentile P, Chiono V, Carmagnola I, Hatton PV. An Overview of Poly(lactic-co-glycolic) Acid (PLGA)-Based Biomaterials for Bone Tissue Engineering. International Journal of Molecular Sciences 2014;15:3640-59.

[4] Sui G, Yang X, Mei F, Hu X, Chen G, Deng X, Ryu, Seungkon. Poly-L-lactic acid/hydroxyapatite hybrid membrane for bone tissue regeneration. Journal of Biomedical Materials Research Part A 2007;82A:445-54.

[5] Madhavan Nampoothiri K, Nair NR, John RP. An overview of the recent developments in polylactide (PLA) research. Bioresource Technology 2010;101:8493-501.

[6] Ren J, Blackwood KA, Doustgani A, Poh PP, Steck R, Stevens MM, Woodruff, Maria A.. Melt-electrospun polycaprolactone-strontium substituted bioactive glass scaffolds for bone regeneration. Journal of Biomedical Materials Research Part A 2013:n/a-n/a.

[7] Gupta B, Revagade N, Hilborn J. Poly(lactic acid) fiber: An overview. Progress in Polymer Science 2007;32:455-82.

[8] Martins A, Duarte ARC, Faria S, Marques AP, Reis RL, Neves NM. Osteogenic induction of hBMSCs by electrospun scaffolds with dexamethasone release functionality. Biomaterials 2010;31:5875-85.

[9] Santocildes-Romero ME, Goodchild RL, Hatton PV, Crawford A, Reaney IM, Miller CA. Preparation of Composite Electrospun Membranes Containing Strontium-Substituted Bioactive Glasses for Bone Tissue Regeneration. Macromolecular Materials and Engineering 2016.

[10] Haimi S, Suuriniemi N, Haaparanta A-M, Ellä V, Lindroos B, Huhtala H, et al. Growth and Osteogenic Differentiation of Adipose Stem Cells on PLA/Bioactive Glass and PLA/β-TCP Scaffolds. Tissue Engineering Part A 2008;15:1473-80.

[11] Bhakta S, Faira P, Salata L, de Oliveira Neto P, Miller C, van Noort R. Determination of relative in vivo osteoconductivity of modified potassium fluorrichterite glass–ceramics compared with 45S5 bioglass. Journal of Materials Science: Materials in Medicine 2012;23:2521-9.

[12] Hench L. The story of Bioglass. Journal of Materials Science: Materials in Medicine 2006;17:967-78.

[13] Mofokeng JP, Luyt AS. Morphology and thermal degradation studies of melt-mixed poly(lactic acid) (PLA)/poly(ε-caprolactone) (PCL) biodegradable polymer blend nanocomposites with TiO2 as filler. Polymer Testing 2015;45:93-100.

[14] Carrasco F, Pagès P, Gámez-Pérez J, Santana OO, Maspoch ML. Processing of poly(lactic acid): Characterization of chemical structure, thermal stability and mechanical properties. Polymer Degradation and Stability 2010;95:116-25.

[15] Niu Y, Guo L, Liu J, Shen H, Su J, An X. Bioactive and degradable scaffolds of the mesoporous bioglass and poly(l-lactide) composite for bone tissue regeneration. Journal of Materials Chemistry B 2015;3:2962-70.

[16] Hench LL. Bioceramics: From Concept to Clinic. Journal of the American Ceramic Society 1991;74:1487-510.

[17] Barros AAA, Alves A, Nunes C, Coimbra MA, Pires RA, Reis RL. Carboxymethylation of ulvan and chitosan and their use as polymeric components of bone cements. Acta Biomaterialia 2013;9:9086-97.

[18] Gomes FO, Pires RA, Reis RL. Aluminum-free glass-ionomer bone cements with enhanced bioactivity and biodegradability. Materials Science and Engineering: C 2013;33:1361-70.

[19] Rabiee SM, Nazparvar N, Azizian M, Vashaee D, Tayebi L. Effect of ion substitution on properties of bioactive glasses: A review. Ceram Int 2015;41:7241-51.
[20] Rahaman MN, Day DE, Sonny Bal B, Fu Q, Jung SB, Bonewald LF. Bioactive glass in tissue engineering. Acta Biomaterialia 2011;7:2355-73.
[21] Pan HB, Zhao XL, Zhang X, Zhang KB, Li LC, Li ZY. Strontium borate glass: potential biomaterial for bone regeneration. J R Soc Interface 2010;7:1025-31.
[22] Huang W, Day D, Kittiratanapiboon K, Rahaman M. Kinetics and mechanisms of the conversion of silicate (45S5), borate, and borosilicate glasses to hydroxyapatite in dilute phosphate solutions. Journal of Materials Science: Materials in Medicine 2006;17:583-96.
[23] Pires RA, Abrahams I, Nunes TG, Hawkes GE. Multinuclear magnetic resonance studies of borosilicate glasses for use in glass ionomer cements: incorporation of CaO and Al2O3. Journal of Materials Chemistry 2006;16:2364-73.
[24] Pires RA, Abrahams I, Nunes TG, Hawkes GE. The role of alumina in aluminoborosilicate glasses for use in glass-ionomer cements. Journal of Materials Chemistry 2009;19:3652-60.
[25] Wang H, Zhao S, Xiao W, Xue J, Shen Y, Zhou J. Influence of Cu doping in borosilicate bioactive glass and the properties of its derived scaffolds. Materials Science and Engineering: C 2016;58:194-203.
[26] Fernandes JS, Martins M, Neves NM, Fernandes MHFV, Reis RL, Pires RA. Intrinsic Antibacterial Borosilicate Glasses for Bone Tissue Engineering Applications. ACS Biomaterials Science & Engineering 2016.
[27] Marie PJ, Ammann P, Boivin G, Rey C. Mechanisms of Action and Therapeutic Potential of Strontium in Bone. Calcified Tissue International 2001;69:121-9.
[28] Hoppe A, Güldal NS, Boccaccini AR. A review of the biological response to ionic dissolution products from bioactive glasses and glass-ceramics. Biomaterials 2011;32:2757-74.
[29] Hesaraki S, Gholami M, Vazehrad S, Shahrabi S. The effect of Sr concentration on bioactivity and biocompatibility of sol–gel derived glasses based on CaO–SrO–SiO2–P2O5 quaternary system. Materials Science and Engineering: C 2010;30:383-90.
[30] Wu C, Fan W, Gelinsky M, Xiao Y, Simon P, Schulze R. Bioactive SrO–SiO2 glass with well-ordered mesopores: Characterization, physiochemistry and biological properties. Acta Biomaterialia 2011;7:1797-806.
[31] Santocildes-Romero ME, Crawford A, Hatton PV, Goodchild RL, Reaney IM, Miller CA. The osteogenic response of mesenchymal stromal cells to strontium-substituted bioactive glasses. Journal of Tissue Engineering and Regenerative Medicine 2015;9:619-31.
[32] Gentleman E, Fredholm YC, Jell G, Lotfibakhshaiesh N, O'Donnell MD, Hill RG. The effects of strontium-substituted bioactive glasses on osteoblasts and osteoclasts in vitro. Biomaterials 2010;31:3949-56.
[33] Brooke G, Cook M, Blair C, Han R, Heazlewood C, Jones B. Therapeutic applications of mesenchymal stromal cells. Seminars in Cell & Developmental Biology 2007;18:846-58.
[34] Maniatopoulos C, Sodek J, Melcher AH. Bone formation in vitro by stromal cells obtained from bone marrow of young adult rats. Cell Tissue Res 1988;254:317-30.
[35] Livak KJ, Schmittgen TD. Analysis of Relative Gene Expression Data Using Real-Time Quantitative PCR and the 2−ΔΔCT Method. Methods 2001;25:402-8.
[36] Rajzer I, Menaszek E, Kwiatkowski R, Chrzanowski W. Bioactive nanocomposite PLDL/nano-hydroxyapatite electrospun membranes for bone tissue engineering. J Mater Sci: Mater Med 2014;25:1239-47.
[37] Chan BP, Leong KW. Scaffolding in tissue engineering: general approaches and tissue-specific considerations. European Spine Journal 2008;17:467-79.
[38] Liang S-L, Cook WD, Thouas GA, Chen Q-Z. The mechanical characteristics and in vitro biocompatibility of poly(glycerol sebacate)-Bioglass® elastomeric composites. Biomaterials 2010;31:8516-29.

663 [39] Thomas V, Jagani S, Johnson K, Jose MV, Dean DR, Vohra YK, et al. Electrospun Bioactive
664 Nanocomposite Scaffolds of Polycaprolactone and Nanohydroxyapatite for Bone Tissue
665 Engineering. Journal of Nanoscience and Nanotechnology 2006;6:487-93.
666 [40] Jeong SI, Ko EK, Yum J, Jung CH, Lee YM, Shin H. Nanofibrous Poly(lactic
667 acid)/Hydroxyapatite Composite Scaffolds for Guided Tissue Regeneration. Macromolecular
668 Bioscience 2008;8:328-38.
669 [41] Shakya AK, Holmdahl R, Nandakumar KS, Kumar A. Polymeric cryogels are biocompatible,
670 and their biodegradation is independent of oxidative radicals. Journal of Biomedical Materials
671 Research Part A 2014;102:3409-18.
672 [42] Liao G, Jiang S, Xu X, Ke Y. Electrospun aligned PLLA/PCL/HA composite fibrous
673 membranes and their in vitro degradation behaviors. Materials Letters 2012;82:159-62.
674 [43] Navarro M, Ginebra MP, Planell JA, Barrias CC, Barbosa MA. In vitro degradation behavior
675 of a novel bioresorbable composite material based on PLA and a soluble CaP glass. Acta
676 Biomaterialia 2005;1:411-9.
677 [44] Zonari A, Novikoff S, Electo NRP, Breyner NM, Gomes DA, Martins A. Endothelial
678 Differentiation of Human Stem Cells Seeded onto Electrospun
679 Polyhydroxybutyrate/Polyhydroxybutyrate-Co-Hydroxyvalerate Fiber Mesh. PLoS ONE
680 2012;7:e35422.
681 [45] Amorim S, Martins A, Neves NM, Reis RL, Pires RA. Hyaluronic acid/poly-l-lysine bilayered
682 silica nanoparticles enhance the osteogenic differentiation of human mesenchymal stem cells.
683 Journal of Materials Chemistry B 2014;2:6939-46.
684 [46] Marie PJ, Fromigué O. Osteogenic differentiation of human marrow-derived mesenchymal
685 stem cells. Regenerative Medicine 2006;1:539-48.
686 [47] Peng S, Zhou G, Luk KDK, Cheung KMC, Li Z, Lam WM. Strontium Promotes Osteogenic
687 Differentiation of Mesenchymal Stem Cells Through the Ras/MAPK Signaling Pathway. Cellular
688 Physiology and Biochemistry 2009;23:165-74.
689 [48] Yang F, Yang D, Tu J, Zheng Q, Cai L, Wang L. Strontium Enhances Osteogenic
690 Differentiation of Mesenchymal Stem Cells and In Vivo Bone Formation by Activating
691 Wnt/Catenin Signaling. STEM CELLS 2011;29:981-91.
692 [49] Kim H-W, Lee H-H, Knowles JC. Electrospinning biomedical nanocomposite fibers of
693 hydroxyapatite/poly(lactic acid) for bone regeneration. Journal of Biomedical Materials
694 Research Part A 2006;79A:643-9.
695 [50] Reis AMS, Ribeiro LGR, Ocarino NdM, Goes AM, Serakides R. Osteogenic potential of
696 osteoblasts from neonatal rats born to mothers treated with caffeine throughout pregnancy.
697 BMC Musculoskeletal Disorders 2015;16:1-11.
698 [51] zur Nieden NI, Kempka G, Ahr HJ. In vitro differentiation of embryonic stem cells into
699 mineralized osteoblasts. Differentiation 2003;71:18-27.
700 [52] Munisso MC, Kang J-H, Tsurufuji M, Yamaoka T. Cilomilast enhances osteoblast
701 differentiation of mesenchymal stem cells and bone formation induced by bone
702 morphogenetic protein 2. Biochimie 2012;94:2360-5.
703 [53] Ashammakhi N, Reis R, Chiellini E. Chapter 13: Genes and Proteins Involved in the
704 Regulation of Osteogenesis. In: G. K, S. C, N. A, editors. Topics in Tissue Engineering2007.
705 [54] Strobel LA, Hild N, Mohn D, Stark WJ, Hoppe A, Gbureck U. Novel strontium-doped
706 bioactive glass nanoparticles enhance proliferation and osteogenic differentiation of human
707 bone marrow stromal cells. Journal of Nanoparticle Research 2013;15:1-9.
708 [55] Tu Q, Valverde P, Chen J. Osterix enhances proliferation and osteogenic potential of bone
709 marrow stromal cells. Biochemical and biophysical research communications 2006;341:1257-
710 65.
711 [56] Isaac J, Nohra J, Isaac J, Jallot E, JNedelec J, Berdal A, et al. Effects of strontium-doped
712 bioactive glass on the differentiation of cultured osteogenic cells. European Cells and Materials
713 2011;21:130-43.